

Excitonic and Phonon-Mediated Optical Stark Effects in a Conjugated Polymer

G. J. Blanchard, J. P. Heritage, A. C. Von Lehmen, M. K. Kelly, G. L. Baker, and S. Etemad
Bell Communications Research, Inc., 331 Newman Springs Road, Red Bank, New Jersey 07701

(Received 17 April 1989)

We have investigated the subresonant optical response of the polydiacetylene PTS using stimulated inverse Raman spectroscopy. The data exhibit energy-dependent line-shape variations which are caused by the optical Stark effect on the exciton-phonon and exciton-ground-state transitions. These are the first observations of *both* phonon-mediated and excitonic optical Stark effects in a 1D conjugated polymer. Excellent agreement is achieved between the data and our calculations using a theory of phonon-mediated changes in susceptibility.

PACS numbers: 78.20.Jq

Conjugated polymers have been studied extensively because of their large optical nonlinearities.¹⁻⁴ There are two reasons for interest in these organic semiconductors: understanding the mechanism(s) of their nonlinear behavior, and their potential application in high-speed optical signal processing technologies.⁵ These materials are model 1D systems. In both these and other reduced-dimensionality systems, anharmonic interactions between excitons and photons determine their *resonant* nonlinear response.^{3,6} Resonant excitation bleaches the exciton uniformly as a result of the Fermi-particle statistics which the electrons and holes must obey. This bleaching is termed "phase-space filling" (PSF) and accounts for the excitonic response observed in GaAs/AlGaAs 2D multiple-quantum-well structures⁷ and PTS, a crystalline polydiacetylene.³

The nonlinear response of reduced-dimension exciton systems to *nonresonant* excitation is dominated by virtual excitons and carriers. These virtual particles exist only when the nonresonant optical excitation field is present. One characteristic signature of nonresonant excitation is the optical Stark shifting of the exciton transition, caused by the anharmonic interactions among virtual particles.⁸ Although the optical Stark effect has been observed in III-V quantum wells, it has not yet been seen in any 1D system.

The nonresonant response of 1D conjugated polymers is expected to contain the same features as that of III-V quantum wells. However, because of their characteristically strong exciton-phonon coupling, conjugated polymers also exhibit an additional nonlinearity. In particular, nonresonant excitation of the model 1D semiconductor PTS produces a "hole" in its exciton absorption.⁸ A splitting of the exciton energy level as a consequence of the strong exciton-phonon coupling has been proposed to explain the existence of the hole. We report in this Letter our small-signal investigation of the subresonant optical response of PTS in a spectral region where strong exciton-phonon coupling dominates the observed nonlinearities and optical Stark effects are clearly evident.

The spectra which we present here reveal three princi-

pal features. The first is the inverse Raman loss spectrum of optical phonons. The second is the response of the exciton to the optical Stark effect for the phonon-exciton transition. We refer to this as the phonon-mediated optical Stark effect (PMOSE). The third feature is the optical Stark shifting of the ground-state-exciton transition, termed the excitonic optical Stark effect. We observe dramatic energy-dependent variations in phonon line shape due to interference between the Raman effect and the phonon-mediated optical Stark effect. Our data are also the first evidence for the excitonic optical Stark effect in a 1D system, analogous to that seen before in 2D systems. The excitonic optical Stark effect becomes evident for excitation sufficiently far from resonance that the phonon-mediated optical Stark effect becomes small. We achieve excellent agreement with the data using the theory of phonon-mediated optical nonlinearities⁸ when the large energy-dependent variations in the complex dielectric constant, $\epsilon_1 + i\epsilon_2$, are accounted for and the excitonic optical Stark effect is included. These data demonstrate collectively the central role that dynamical Stark effects play in determining PTS's nonlinear optical response.

Thin single crystals of PTS⁹ were studied using stimulated inverse Raman spectroscopy (SIRS).¹⁰ The spectrometer used here has been described elsewhere.¹¹ The Stokes (pump) beam intensity was 10^7 W/cm² and the anti-Stokes (probe) intensity was 10^5 W/cm², calculated from the measured power and spot size at the sample. The low probe intensity perturbed the excitonic system negligibly. The transient signals persisted only while the pump and probe pulses were coincident in time. The temporal resolution of this system is ~ 10 ps FWHM and the bandwidth of each laser is 2.7 cm⁻¹. A series of Raman spectra were taken at 298 K at a progression of pump energies. For each pump energy the probe was varied over a spectral region containing the exciton and at least one phonon resonance.

PTS exhibits an intense exciton absorption, shown in Fig. 1(a). For a strongly absorbing system, the transmission spectrum does not measure the exciton line

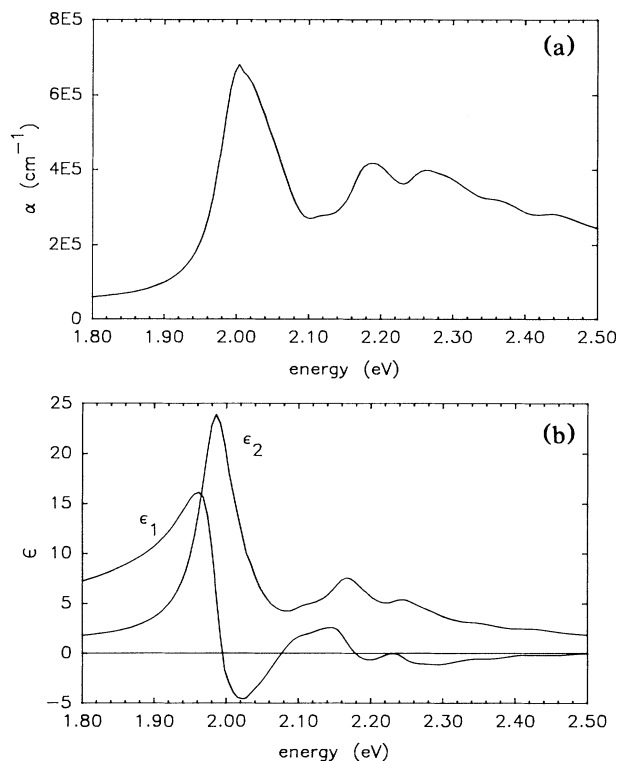


FIG. 1. (a) The linear absorption spectrum of PTS at 300 K, calculated from the ellipsometric data. The apparent line-width is 110 meV. (b) Ellipsometric measurement of PTS's complex dielectric response parallel to its chain axis. The ϵ_2 linewidth is 60 meV.

shape directly. Ellipsometric measurement of PTS [Fig. 1(b)] shows the width of the exciton to be substantially less than that shown in Fig. 1(a). The ϵ_2 line has a width of $2\gamma_x = 60$ meV and is located at 1.984 eV rather than 2 eV.

We present in Fig. 2 a series of inverse Raman spectra for a progression of pump energies. Both the ω_1 (0.184 eV, C=C stretch) and ω_2 (0.258 eV, C≡C stretch) phonon resonances track with the pump photon energy. There are two noteworthy features shown in Fig. 2. The first is the significant phonon line-shape change as a function of overlap with the exciton resonance. This effect is apparent for both phonons. At $\omega_p = 1.699$ eV, $\omega_p + \omega_2 = 1.957$ eV, 27 meV below the exciton, and the ω_2 line shape is absorptive; at $\omega_p = 1.753$ eV the line shape is transmissive, and between these two limits the ω_2 line assumes a dispersive shape. The transmissive ω_1 resonance ($\omega_p = 1.816$ eV) is the hole reported previously.⁸ The second feature, seen for $\omega_p = 1.699$, 1.713, and 1.720 eV, is a zero crossing near 2 eV corresponding to an exciton blue shift.

The essential physics underlying these spectra can be understood by examining $\chi^{(3)}$ for this system.^{12,13} $\chi^{(3)}(\omega_{pr}, \omega_p, \omega, -\omega, \omega_{pr})$ represents the nonlinear response

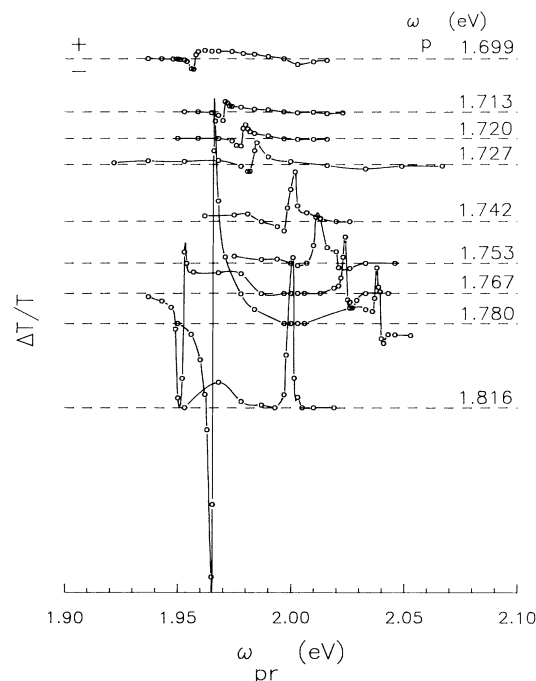


FIG. 2. Inverse Raman spectra of the ω_1 (0.184 eV) and ω_2 (0.258 eV) phonons at a progression of pump energies, listed on the right-hand side. Each point in these spectra represents the average intensity from at least three individual time-resolved scans.

of the sample to ω_p at ω_{pr} ,

$$\chi^{(3)} \propto \frac{\langle 0 | \mu_x^2 | X \rangle \langle X | \mu_1^2 | 1 \rangle \langle 1 | \mu_1^2 | X \rangle \langle X | \mu_x^2 | 0 \rangle}{(\omega_x - \omega_{pr} - i\gamma_x)^2 [\omega_1 - (\omega_{pr} - \omega_p) - i\gamma_1]}, \quad (1)$$

where $|0\rangle$, $|1\rangle$, and $|X\rangle$ refer to the ground state, phonon, and exciton, respectively, and μ_x and μ_1 are the exciton-ground-state and exciton-phonon transition moments, respectively. Two limiting cases describe the important features. For pumping below the exciton resonance but on the Raman resonance, $\omega_p + \omega_1 \ll \omega_x$ and $\omega_{pr} - \omega_p = \omega_1$. The term $\omega_1 - (\omega_{pr} - \omega_p) - i\gamma_1$ determines the response and produces an absorptive resonance in $\text{Im}\{\chi^{(3)}\}$ corresponding to the Raman transition. In the vicinity of the double resonance, where ω_{pr} is tuned through ω_x and $\omega_p + \omega_1 = \omega_x$, the real terms in the denominator of Eq. (1) approach zero and give rise to a transmissive imaginary response which corresponds to Stark splitting of the exciton resonance. Between these two limiting cases, both terms in the denominator contribute to produce the dispersive line shapes, characteristic of interference between the Raman effect and the phonon-mediated optical Stark effect. The PMOSE is analogous to the resonant optical Stark effect for a cou-

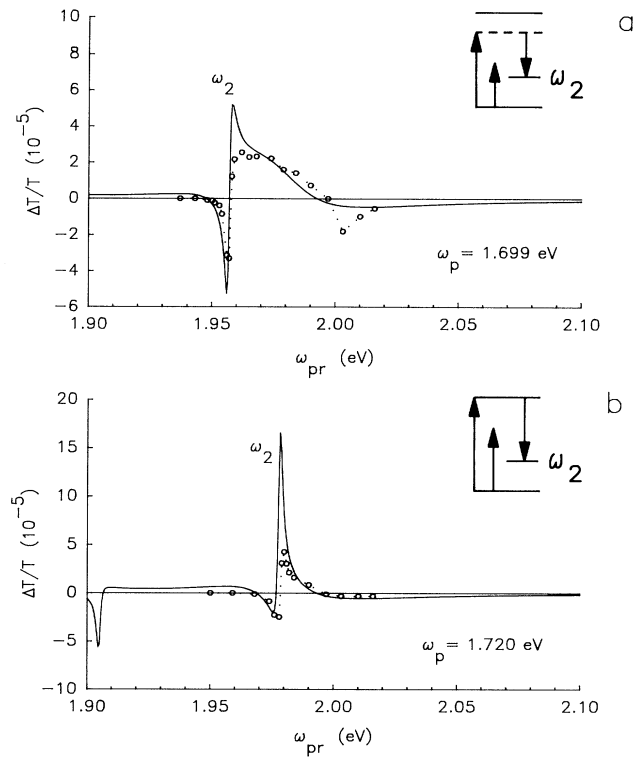


FIG. 3. (a) Experimental and calculated SIRS spectra for $\omega_p = 1.699$ eV. (b) Experimental and calculated SIRS spectra for $\omega_p = 1.720$ eV. The points are experimental data and the lines are the calculated response.

pled three-level system, observed in Cu_2O .¹³ The excitonic optical Stark effect has been observed before in quantum wells, but not in PTS. We find that both contribute to the off-resonance response of PTS, but the PMOSE dominates near the region where the pump and phonon energies add together to approach the exciton energy.

While $\chi^{(3)}$ is useful in understanding the relevant spectroscopy, we have used a more complete theory for our calculations.^{8,14} It includes many-body effects, is valid for all pump and probe powers, and, in the small-signal limit, reduces to $\chi^{(3)}$. We have calculated the total nonlinear susceptibility experienced by the probe, χ_{pr} , including the explicit self-energy terms. The original model⁸ includes only one phonon and does not consider the excitonic optical Stark effect. In our calculation we have incorporated two phonons via a linear superposition and have also included the excitonic optical Stark effect by approximating the exciton frequency to be

$$\omega_x \approx \omega_x^0 + R^2 / (\omega_x^0 - \omega_p), \quad (2)$$

where ω_x^0 is the unperturbed exciton resonance and R ($=\mu_x E_p = 4 \times 10^{-4}$ eV) is the Rabi frequency. Inclusion of the excitonic Stark effect is necessary to achieve quantitative agreement with the off-resonance data. We

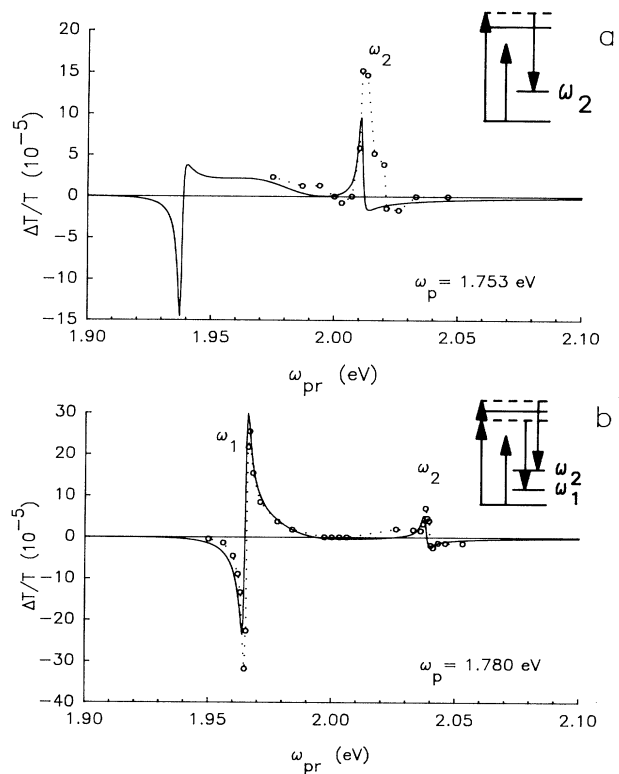


FIG. 4. (a) Experimental and calculated SIRS spectra for $\omega_p = 1.753$ eV. (b) Experimental and calculated SIRS spectra for $\omega_p = 1.780$ eV. The points are experimental data and the lines are the calculated response.

detect experimentally the quantity $\Delta T/T$. For small signals and samples sufficiently thick that energy-dependent variations in their interface reflections may be neglected, $\Delta T/T \approx \Delta a l = (2\omega l/c)\Delta k$, where Δk is the change in extinction coefficient due to the presence of the pump. Because $\epsilon_1 = 1 + 4\pi \text{Re}\{\chi_{pr}\}$ and $\epsilon_2 = 4\pi \text{Im}\{\chi_{pr}\}$ are large and vary by a factor of 10 over the exciton resonance [Fig. 1(b)], calculation of the extinction coefficient $k = \{(\epsilon_1^2 + \epsilon_2^2)^{1/2} - \epsilon_1\}^{1/2}$ yields more precise agreement with the data than does a simple comparison to χ_{pr} . In our calculations $l = 600$ Å and the exciton-phonon coupling constants are determined from data in Ref. 15.

The quantitative agreement between data and theory is presented in Figs. 3 and 4. The calculated pump-energy-dependent line shapes are reproduced for both phonons, progressing from absorptive through dispersive to transmissive to reverse-dispersive as the phonon is "scanned" across the exciton. Detailed examination of four spectra demonstrates the agreement. A schematic energy-level diagram showing the appropriate photon energies and three-level system is inset in each figure. For $\omega_p = 1.699$ eV [Fig. 3(a)], the data show a predominantly absorptive ω_2 phonon line shape and a blue shift of the

exciton. The calculated spectrum shows a slightly dispersive phonon line shape with the same zero crossing. This zero crossing can be traced to the excitonic optical Stark effect while the phonon line shape is dominated by the PMOSE. As resonance is approached ($\omega_p = \omega_x - \omega_i$), the PMOSE becomes dominant over the excitonic Stark effect. The latter remains small due to PTS's high phonon energies. For $\omega_p = 1.720$ eV [Fig. 3(b)], ω_2 is in exact resonance with ω_x^0 . The dispersive spectrum is predicted by the calculation as is the zero crossing at 2 eV. At exact resonance, χ_{pr} is calculated to be transmissive. Contributions from ϵ_1 and ϵ_2 produce the observed dispersive line shape. For both Figs. 3(a) and 3(b), the ω_2 phonon line shape is calculated to be too transmissive because the assumed Lorentzian wings do not fall off as rapidly as the actual exciton absorption profile.

Two spectra are presented in Fig. 4, where $\omega_2 + \omega_p > \omega_x$. For $\omega_p = 1.753$ eV [Fig. 4(a)] the calculated line shape tracks the data closely but produces a feature too narrow. For $\omega_p = 1.780$ eV [Fig. 4(b)], the ω_1 phonon is near resonance, with the ω_2 phonon 54 meV above ω_x^0 . In addition to the line-shape agreement for this spectrum, the relative intensity of each phonon is reproduced. We have estimated our sample thickness to be 600 Å in all calculations.^{1,9,16} The actual thickness of individual crystals used in each experiment varied by a small, undetermined amount. This is the source of the slight difference between the calculated and experimental *intensities* in Figs. 3(b) and 4(a).

In conclusion, we report the first observation of the phonon-mediated optical Stark effect (PMOSE) in a 1D organic semiconductor. This effect is predicted and modeled well by a theory which allows for strong exciton-phonon coupling. The phonon-mediated optical Stark effect is of central importance in PTS due to strong exciton-phonon coupling. The quantitative agreement between the theory of the phonon-mediated change in the susceptibility [$\Delta\chi(\omega)$]⁸ and the measured changes in the extinction spectra [$\Delta k(\omega)$] verifies the validity of this theory in the small-signal limit. The higher-order nonlinear effects which it predicts remain to be investigated experimentally. In the small-signal limit, the dynamic Stark shifting and splitting of the exciton

← ground-state and exciton ← phonon transitions together determine the nonlinear optical response of PTS. Despite the complexity of this conjugated polymer system, *nonresonant* small-signal optical nonlinearities can be treated effectively as a superposition of coupled three-level systems.

We thank D. S. Chemla and S. Schmitt-Rink for several insightful discussions and D. E. Aspnes for assistance in interpreting the ellipsometric results.

¹G. J. Blanchard, J. P. Heritage, G. L. Baker, and S. Etamad, Chem. Phys. Lett. **158**, 329 (1989).

²G. M. Carter, M. K. Thakur, Y. J. Chen, and J. V. Hryniewicz, Appl. Phys. Lett. **47**, 457 (1985).

³B. I. Greene, J. Orenstein, R. R. Millard, and L. R. Williams, Phys. Rev. Lett. **58**, 2750 (1987).

⁴B. I. Greene, J. Orenstein, R. R. Millard, and L. R. Williams, Chem. Phys. Lett. **139**, 381 (1987).

⁵P. W. Smith, Bell Syst. Tech. J. **61**, 1975 (1982).

⁶See, for example, S. Schmitt-Rink, D. S. Chemla, and D. A. B. Miller, Adv. Phys. (to be published).

⁷A. Von Lehmen, D. S. Chemla, J. E. Zucker, and J. P. Heritage, Opt. Lett. **11**, 609 (1986).

⁸B. I. Greene, J. F. Mueller, J. Orenstein, D. H. Rapkine, S. Schmitt-Rink, and M. Thakur, Phys. Rev. Lett. **61**, 325 (1988).

⁹M. K. Thakur and S. E. Meyler, Macromolecules **18**, 2341 (1985).

¹⁰W. J. Jones and B. P. Stoicheff, Phys. Rev. Lett. **13**, 657 (1964).

¹¹G. J. Blanchard, J. Chem. Phys. **87**, 6802 (1987).

¹²S. Saikan, N. Hashimoto, T. Kushida, and K. Namba, J. Chem. Phys. **82**, 5409 (1985).

¹³D. Frolich, A. Nothe, and K. Reimann, Phys. Rev. Lett. **55**, 1335 (1985).

¹⁴B. I. Greene, J. Orenstein, S. Schmitt-Rink, and M. Thakur, in *Proceedings of the NATO Workshop on Optical Switching in Low-Dimensional Systems, Marbella, Spain, 1988*, edited by H. Haug and L. Banyal, NATO Advanced Study Institutes, Ser. B Vol. 194 (Plenum, New York, 1989).

¹⁵D. N. Batchelder and D. Bloor, J. Phys. C **15**, 3005 (1982).

¹⁶R. R. Chance and R. H. Baughman, J. Chem. Phys. **64**, 3889 (1976).